JOURNAL OF MATERIALS SCIENCE 5 (1970) 434–444

The Activation Areas for Creep Deformation

N. BALASUBRAMANIAN*
Henry Krumb School of Mines, Columbia University, New York, USA

J. C. M. LI*
E. C. Bain Laboratory for Fundamental Research, US Steel Corporation, Monroeville, Pennsylvania, USA

The activation areas for creep deformation are collected and examined in the light of many material and deformation variables. The activation area is $A^* = (kT/\mathbf{b})\,(\partial \ln\dot{\epsilon}/\partial\tau^*)_T$ where k is Boltzmann's constant, T the absolute temperature, $\mathbf{b}$ the Burgers vector, $\dot{\epsilon}$ the steady state creep rate, and τ^* the effective shear stress. It is found that within a factor of 5, there is a general correlation between activation area and stress for all metals, alloys, semiconductors and ionic crystals. A jog-limited dislocation motion with a distribution of jog spacings is suggested as a possible mechanism for this behaviour. Some limitations for the jog mechanism are discussed.

1. Introduction

The concept of thermally activated processes has been very helpful in the investigations of rate-controlling mechanisms of plastic deformation. For instance, activation enthalpy and its stress-dependence [1, 2] are used extensively in low-temperature deformation to compare with various mechanisms such as Peierls mechanism, impurity mechanism and intersection mechanism. In high-temperature creep, however, the concept of thermal activation is only partially applied in the sense that the contribution of stress to the activation process is neglected. The activation enthalpy [3] and activation volume [4, 5] for creep have been shown to equal those for self-diffusion. As a consequence, it is now a requirement for all theories of creep that self-diffusion be considered the rate-controlling step. Both these activation parameters are calculated assuming constant dislocation structure, i.e. the effect of temperature and pressure is assumed not to cause any dislocation rearrangement. The effect of stress on the other hand is considered in all existing theories of creep to change the dislocation structure. It is not obvious why the dislocation structure should respond instantly to stress and not to temperature and pressure. Following the practice in low-temperature deformation, in this paper the dislocation structure is assumed to remain essentially constant during a change of temperature, pressure, or stress. The analysis is identical to that of low-temperature deformation and is described as follows:

The creep rate is expressed as

$$\dot{\epsilon} = \dot{\epsilon}_c \exp(-\Delta F^{\ddagger}/kT) \qquad (1)$$

where $\Delta F^{\ddagger}$ is the standard free energy of activation, $\dot{\epsilon}_c$ is the maximum attainable creep rate at $\Delta F^{\ddagger} = 0$, k is the Boltzmann constant and T is absolute temperature. In terms of a dislocation mechanism, $\dot{\epsilon}_c$ contains the density of mobile dislocations, a gemoteric factor, and the maximum attainable velocity at $\Delta F^{\ddagger} = 0$.

Based on the assumption of a single rate process represented by equation 1, the temperature, pressure, and the stress-dependence of creep rate are related to the following activation parameters:

$$\frac{\partial \ln \dot{\epsilon}}{\partial T} = \frac{1}{kT^2}\frac{\partial(\Delta F^{\ddagger}/T)}{\partial(1/T)} = \frac{\Delta H^{\ddagger}}{kT^2}; \qquad (2)$$

$$\frac{\partial \ln \dot{\epsilon}}{\partial P} = -\frac{1}{kT}\frac{\partial \Delta F^{\ddagger}}{\partial P} = -\frac{\Delta V^{\ddagger}}{kT}; \qquad (3)$$

$$\frac{\partial \ln \dot{\epsilon}}{\partial \tau^*} = -\frac{1}{kT}\frac{\partial \Delta F^{\ddagger}}{\partial \tau^*} = \frac{A^*\mathbf{b}}{kT}; \qquad (4)$$

* Now at Materials Research Centre, Allied Chemical Corporation, Morristown, New Jersey, USA.

where $\Delta H^{\ddagger}$ is the activation enthalpy, $\Delta V^{\ddagger}$ is the activation volume, A^* is the activation area, and **b** is the Burgers vector of the dislocation. In deriving these equations, two assumptions have been made: (i) The quantity $\dot{\epsilon}_c$ is regarded as constant and independent of temperature, pressure, or stress. If this is not so, $\dot{\epsilon}$ should be replaced by $\dot{\epsilon}/\dot{\epsilon}_c$ in equations 2, 3 and 4. (ii) The creep rate should be so high that the rate in the reverse direction may be neglected. This will be discussed in more detail later.

The quantity $A^*\mathbf{b}$ is unfortunately also called the activation volume in low-temperature deformation. To avoid confusion with the pressure derivative of the activation free energy, the quantity A^* is here called the activation area, to be discussed in detail later. While the activation enthalpy and the activation volume are well-accepted quantities in creep, the activation area has not been used, despite the fact that it is widely used in low-temperature deformation (under the name activation volume). It is the purpose of this paper to explore this quantity in high-temperature creep ($T > T_m/2$) but not in the range of Nabarro-Herring creep [6, 7].

2. The Activation Area

It is suggested by equation 4 that the applied stress can contribute to the activation free energy. Exactly how this is so depends on the details of the mechanism. For example, in Nabarro-Herring [6, 7] creep, the mechanism is the motion of vacancies between sources and sinks. The external stress changes the free energy, or the chemical potential of vacancies by an amount σV where σ is the normal stress and V is the atomic volume. According to this mechanism, the quantity $A^*\mathbf{b}$ should be of the order of atomic volume.

On the other hand, if the creep mechanism is due to the motion of dislocations, the external stress can contribute to the activation free energy by helping the dislocation to cross the energy barrier. This process is illustrated in fig. 1 for a jog mechanism. The nature of the barrier is immaterial for this illustration. The jogs are indicated by short dotted segments to show that they are not in the slip plane of the dislocation. The circles are vacancies about to be absorbed or emitted. The dislocation segment between the jogs is assumed free and flexible so that it displays a curvature consistent with the shear stress applied in the slip plane.

The free energy of the dislocation is shown schematically in fig. 1 as a function of its position designated as the area swept by the dislocation from its rest configuration at zero stress. The free energy is for that portion of the dislocation which associates with and contributes to the overcoming of one jog barrier. Since the dislocation is passing over a barrier (dragging a jog, slipping past an impurity atom, cutting another dislocation, crossing the Peierls hill, etc.) its free energy must increase in the vicinity of the barrier, reach a maximum, and then decrease after it passes over the barrier. If this process is achieved reversibly by the external stress, the shear stress is proportional to the slope of the free energy-area curve, since $\tau^*\mathbf{b}dA$ is the reversible work done by the shear stress τ^* while the dislocation sweeps an infinitesimal area dA. The shear stress to maintain any dislocation position is thus also a function of the area swept by the dislocation from its rest configuration at zero stress as shown in fig. 1.

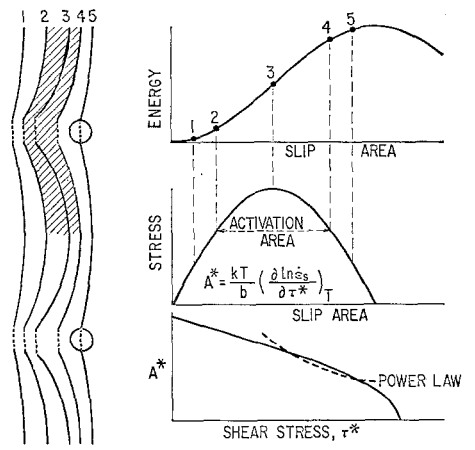

Figure 1 Schematic illustration of activation area in a jog mechanism of creep.

Frequently the thermally-activated dislocation process is described in terms of a force-distance relation at the barrier. The activation area is then given by xL where x is the distance moved by the dislocation at the barrier and L is the length of the segment between barriers. However, this formulation is strictly true only for straight dislocations or at most for a situation in which the shape of the dislocation segment between barriers is independent of stress. To deal with a more realistic situation in which the curvature of the segment between barriers may depend on the applied stress, the area swept by

the portion of the dislocation which is directly involved in the overcoming of the barrier, is used to define the position of the dislocation instead of the distance advanced at the barrier.

Let us suppose that the external stress is sufficient only to maintain the dislocation configuration at position 2 in fig. 1. In order to pass over the barrier, the dislocation must receive an amount of activation free energy sufficient to bring it to position 4 after which the dislocation can pass over the barrier by the external stress alone. The area swept by the dislocation between the positions 2 and 4 (shaded area in fig. 1) for each activation event is defined as the activation area, A^*. (It may be worth mentioning here that this is not the area swept by the dislocation after the activation process.) It is seen from the foregoing considerations that

$$\Delta F^{\ddagger} = \mathbf{b} \int_{\tau^*}^{\tau_c^*} A^* \mathrm{d}\tau^* \qquad (5)$$

where τ_c^* is the maximum shear stress, namely, that required to maintain the dislocation at position 3. Equation 5 shows that

$$\partial \Delta F^{\ddagger} / \partial \tau^* = -A^* \mathbf{b} \qquad (6)$$

which is another definition of activation area. The fact that the activation area is not a constant and must depend on the stress is quite obvious from fig. 1 for any reasonable free energy-area relationship.

Equation 5 can be rewritten as

$$\Delta F^{\ddagger} = \Delta F_0^{\ddagger} - \mathbf{b} \int_0^{\tau^*} A^* \mathrm{d}\tau^* \qquad (7)$$

where $\Delta F_0^{\ddagger}$ is $\Delta F^{\ddagger}$ at $\tau^* = 0$. For very small τ^* so that A^* is nearly the same as A_0^* at $\tau^* = 0$,

$$\Delta F^{\ddagger} = \Delta F_0^{\ddagger} - \mathbf{b}\tau^* A_0^* \,. \qquad (8)$$

A substitution of equation 1 into equation 8 suggests that the forward rate is increased by a factor exp ($\mathbf{b}\tau^* A^*/kT$) from the normal vibration rate of the dislocation and that the reverse rate is decreased by a factor of exp ($-\mathbf{b}\tau^* A^*/kT$). The net creep rate is then

$$\dot{\epsilon} = 2\dot{\epsilon}_0 \exp\left(-\Delta F_0^{\ddagger}/kT\right) \sinh \frac{\mathbf{b}\tau^* A^*}{kT} \qquad (9)$$

which has the following stress-dependence:

$$\frac{\partial \ln \dot{\epsilon}}{\partial \tau^*} = \frac{\mathbf{b}A^*}{kT} \coth \frac{\mathbf{b}\tau^* A^*}{kT} \,. \qquad (10)$$

It is seen that equation 10 agrees with equation 4 only if $\mathbf{b}\tau^* A^*/kT$ is sufficiently large so that the hyperbolic cotangent function is nearly unity. Otherwise a correction has to be made as shown in fig. 2. When $m = \partial \ln \dot{\epsilon}/\partial \ln \tau^*$ is nearly unity, it is not possible to determine A^* accurately. Therefore, this analysis breaks down in the range of Nabarro-Herring creep. Fortunately, in most creep studies, $m > 2$, then equation 4 is applicable.

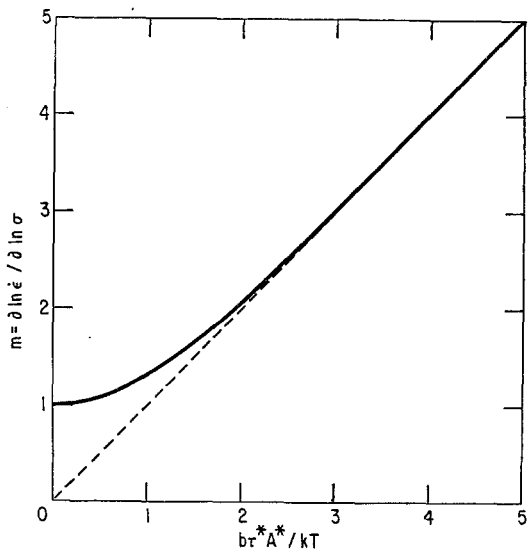

Figure 2 Calculation of activation area from the stress-dependence of creep rate, equation 10.

3. The Effect of Material and Deformation Variables on the Activation Area

The activation area for secondary creep is calculated using equation 4 from literature data on the stress-dependence of creep rate and plotted as a function of applied shear stress in figs. 3 to 14. For polycrystals one-half of the tensile stress is used. In all these calculations an internal stress, τ_i has to be subtracted from the applied stress, τ, to get the effective stress τ^* and the activation area must be expressed as a function of effective stress. Li [5] has shown that in the presence of internal stress the apparent activation area is higher than the true activation area. Hence a correction for internal stress would lower all curves. This will be explicitly shown in the case of stainless steel where the only available data on internal stress for high-temperature creep have been obtained recently by Cuddy [8].

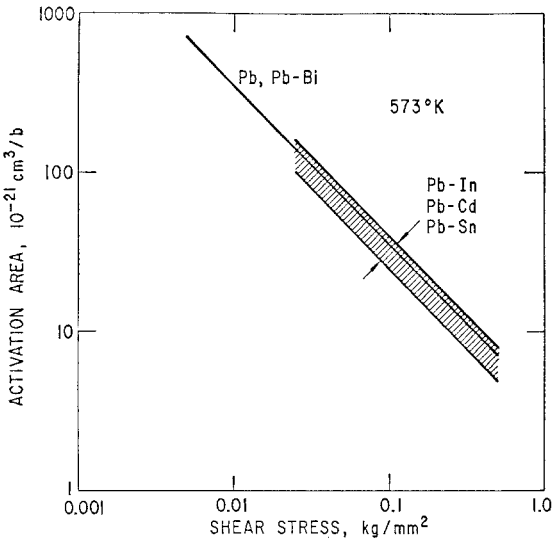

Figure 3 Activation area for the creep of lead and lead alloys. Pb (0.5 to 16% Bi) grain size 0.3 to 2 mm; Pb (3.5 to 31% In) 0.3 to 2 mm; Pb (1.8 to 4.8% Cd) 0.05 to 2 mm; Pb (4.4 to 19% Sn) 0.3 to 2 mm; pure Pb, single crystal.

3.1. Pb and Pb Alloys, Effect of Composition and Grain Size

Fig. 3 shows the activation areas for single crystal Pb and polycrystalline Pb alloys of grain sizes ranging between 0.05 and 2 mm. The activation areas are calculated from Weertman's data at 573° K [9]. It is seen that the activation area is a strong function of stress, but is only weakly dependent on composition or grain size within the range studied. The exact relation between activation area and stress depends on the shape of the energy barrier as shown in fig. 1. The inverse proportionality between activation area and stress in fig. 3 is a consequence of the experimentally observed power law relation between secondary creep rate and stress in the particular range of stress investigated. The present treatment, however, is not restricted to cases where such a power law is obeyed. Alternate relationships between creep rate and stress and consequently between activation area and stress are discussed later in this paper.

3.2. Al and Al–Mg Alloys, Effect of Composition and Temperature

Fig. 4 shows the activation areas for Al and Al–Mg alloys. For Al, Weertman [10] obtained data in the temperature range 430 to 890° K. Harper and Dorn [11] extended the investigation

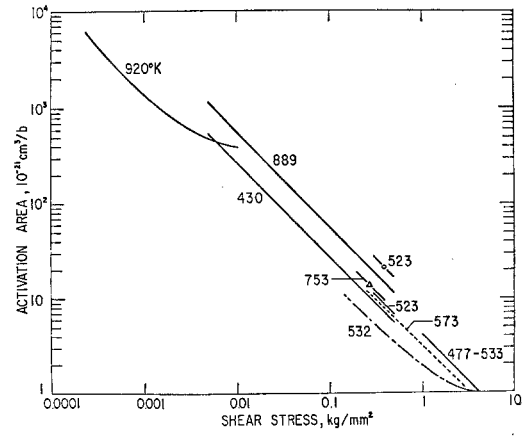

Figure 4 Activation area for the creep of aluminium and aluminium alloys. ——, aluminium; — △ —, aluminium 11% Mg; – – – –, aluminium 2% Mg; — - —, aluminium 3.1% Mg; — ○ —, aluminium stress-cycling.

to 920° K close to the melting point, and this enabled them to obtain data at stresses down to 0.0025 kg mm^{-2}. Data at lower temperatures, 477 to 533° K, were obtained by Servi and Grant [12]. More recently Mitra and McLean [13] obtained data at 523° K both by stress-cycling and in the usual way of running steady state tests on individual specimens at different stresses. The activation areas are lower in the latter case.

For Al–Mg alloys, Laks *et al* [14] studied Al–1.1% Mg alloy at 753° K. Dushman *et al* [15] studied Al–2% Mg alloy at 573° K and Dorn [16] reported on Al–3.1% Mg alloy at 532° K.

It is seen from fig. 4 that the activation area depends more on stress than on temperature or composition.

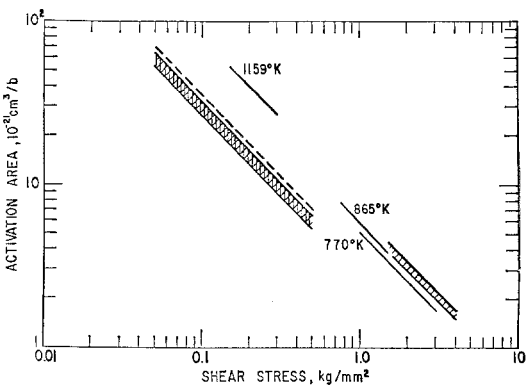

Figure 5 Activation area for the creep of copper and brass: ——, copper; vertical hatching, α-brass, 856 to 973° K; diagonal hatching, β-brass (ordered) 603 to 723° K; – – – –, β-brass (disordered) 759 to 779° K.

3.3. Cu and Brasses, Effect of Stacking Fault Energy and Long Range Order

Fig. 5 shows the activation areas for Cu and Cu–Zn alloys. For Cu, Barrett and Sherby [17] studied the temperature range 770 to 1159° K. The activation areas calculated from the data of Feltham and Meakin [18] between 673 and 973° K were presented [5] before* and agreed well with those of Barrett and Sherby. To study the effect of stacking fault energy on creep, Bonesteel and Sherby [19] investigated α-brasses with 10, 20, and 30% Zn in the temperature range 825 to 973° K and Feltham and Copley [20] studied the same brasses between 823 and 873° K. It is seen from fig. 5 that the activation areas do not depend on stacking fault energy although the creep rates do. The effect of ordering on the creep of β-brasses of 50% Zn was examined by Herman and Brown [21] in the stress range 0.05 to 0.5 kg mm^{-2} and the temperature range 603 to 770° K. More recently Brown and Lenton [22] repeated these experiments in single crystals and their data are included in fig. 5 also. It is seen that the activation areas are not affected by long-range order even though the creep rates are.

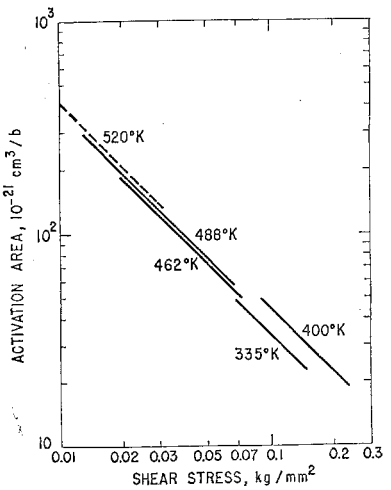

Figure 6 Activation area for the creep of thallium; data of O. D. Sherby. ——, α-Tl; – – –, β-Tl.

3.4. α and β–Tl, Effect of Crystal Structure

Fig. 6 shows the activation areas for α and β-Tl calculated from the data of Sherby [23]. The temperature range 335 to 525° K covers both the hcp and bcc phases, since the transformation temperature is 503° K. It is seen from fig. 6 that the effect of crystal structure on the activation area is small.

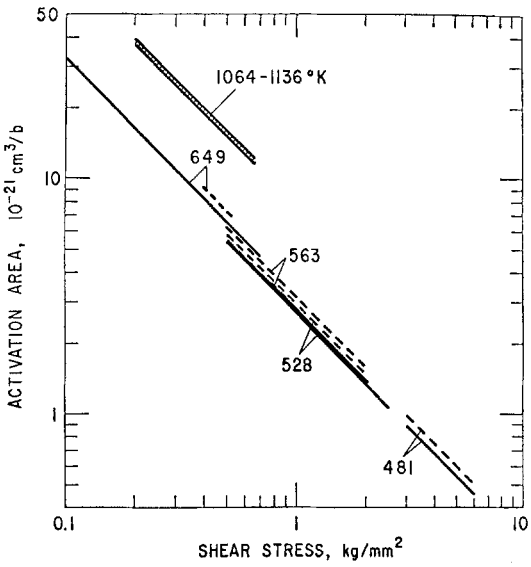

Figure 7 Activation area for the creep of silver and silver alloys: vertical hatched area, Ag polycrystals; ——, Ag 33% Al; – – –, Ag 33% Al 1% Zn.

3.5. Ag and Ag Alloys, Effect of High Concentration

Fig. 7 shows the activation areas for Ag and Ag alloys. Spectroscopically pure (99.97%) silver with an average grain size of 0.21 mm was studied by Munson and Huggins [24] at 1064 to 1136° K using a constant load technique. Prismatic slip in single crystals of Ag–33% Al and Ag–33% Al–1% Zn alloys was studied by Howard *et al* [25] at 481 to 649° K. It is seen that despite the difference in temperature, grain size, crystal structure, and composition, the activation area differs by less than a factor of 3.

3.6. Ni and Ni Alloys, Effect of Magnetic Transformation

Fig. 8 shows the activation areas for Ni and Ni alloys. For Ni the data of Weertman and Shahnian [26] at 1373° K and those of Dennison *et al* [27] at 873° K are used. The latter authors obtained data also on Ni–Cr alloys with 1.1 to

* We take this opportunity to correct some errors in [5]. In figs. 4 and 5, the activation areas should be multiplied by a factor of 4. On p. 98, third line below fig. 5, $20b^2$ should be $80b^2$. In equation 34, the T outside the parentheses should be moved up so it multiplies the quantity in the parentheses.

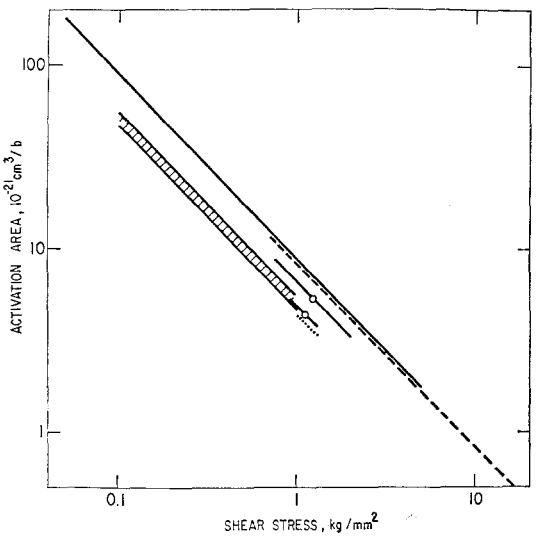

Figure 8 Activation area for the creep of nickel and nickel alloys: vertical hatched area, Ni (13 to 90% Au), 1133° K; . . . . . Ni_3Fe, 840 to 964° K; —— Ni, 1373° K, 873° K; Au, 1133° K; – – – Ni (1.1 to 28.8% Cr), 873° K; —○—, $Ni_{80}Fe_{20}$, 840 to 964° K.

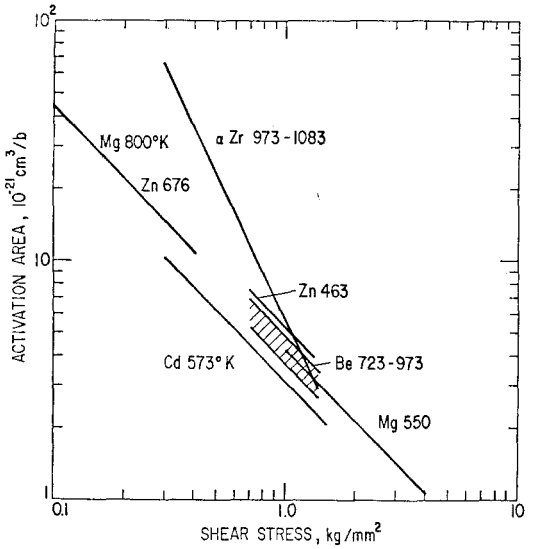

Figure 9 Activation area for the creep of hexagonal metals.

28.8% Cr at 873° K. Sellars and Quarrell [28] studied Ni–Au alloys for the entire range of composition at 1133° K.

Pampillo and Vidoz [29] observed the creep behaviour of Ni_3Fe and $Ni_{80}Fe_{20}$ alloys at 840 to 964° K. The magnetic Curie temperatures for these alloys are 843° K and 880° K, respectively. For the $Ni_{80}Fe_{20}$ alloy, the activation area shows a slight increase across the Curie point, while no change is noticeable for the Ni_3Fe alloy. It is interesting to note that there is no change in activation enthalpy across the Curie point in either alloy.

3.7. Hexagonal Metals, Zn, Mg, Cd, Be, and α–Zr

Fig. 9 shows the activation areas for hexagonal metals. For Zn, the data are from Tegart and Sherby [30], Tegart [31], and Flinn and Munson [32]. For Mg, the data are from Tegart [31] at both 550 and 800° K. The data on Cd are from Flinn and Duran [33]. Bennett and Summer [34] obtained data on Be. For α-Zr, Ardell and Sherby [35] observed some unusual stress-dependence of creep rate. Ardell [36] rationalised in terms of a kink mechanism proposed by Gilman [37] by showing that $\ln\dot{\epsilon}$ is linear with $1/\sigma$. As pointed out by Li [5] such a linear relation implies that the activation area is inversely proportional to the square of stress as opposed to a simple inverse proportionality which leads to the usual power law. This is confirmed in fig. 9. However, the activation areas for α-Zr are somewhat different from those for other hcp metals. In a smaller stress range, and 795 to 893° K Bernstein [38] also obtained creep data on α-Zr which agree with those of Ardell and Sherby [35].

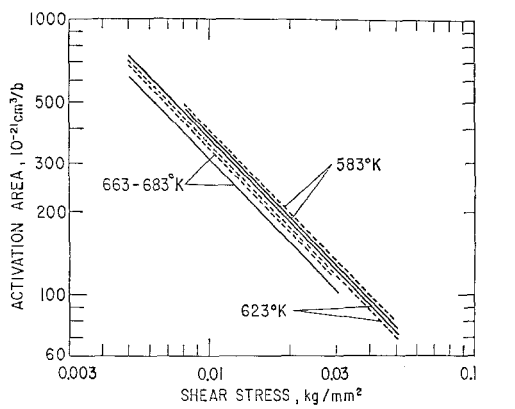

Figure 10 Activation area for the creep of silver bromide; data of R. W. Christy. AgBr single crystals: ——, [001] compression; – – – –, [111] compression.

3.8. AgBr Single Crystals, Effect of Crystal Orientation

Fig. 10 shows the activation areas for AgBr single crystals compressed along <001> and <111> directions based on the data of Christy [39] at 583 to 683° K. It is seen that there is no

definite effect of the direction of compression on the activation area.

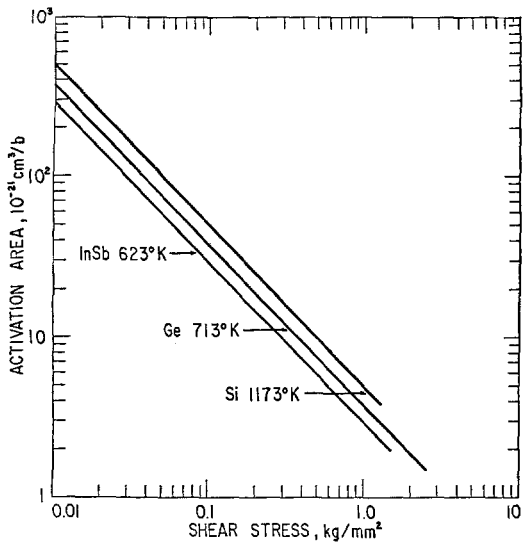

Figure 11 Activation area for creep of semiconductors. InSb, Peissker, Haasen and Alexander; Ge, Penning and de Wind; Si, Reppich.

3.9. Semiconductors, Ge, Si, and InSb

Fig. 11 shows the activation areas for semiconductor crystals. The data on Ge and Si are taken from Haasen [40] and those on InSb are from Peissker *et al* [41].

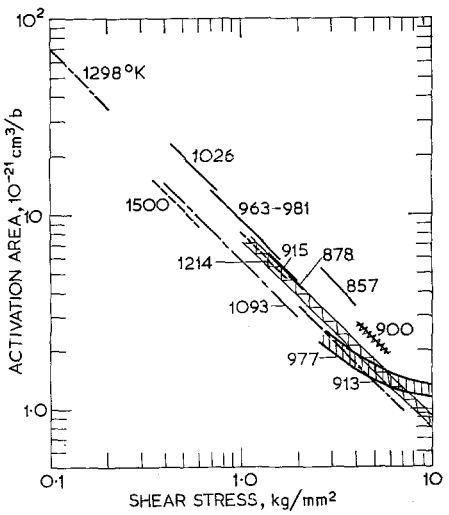

Figure 12 Activation area for the creep of iron and steel: ——, αFe; – – – –, γFe; — · —, Fe 3.1% Si; ⁂, Fe 25.5% Al; area of vertical hatching, austenitic Fe base alloy; area of diagonal hatching, 304 steel.

3.10. Fe, Fe-Si Fe-Al, and Other Iron Alloys

Fig. 12 shows the activation areas for iron and steel. For α-Fe, Ishida *et al* [42] studied in the stress range of 0.5 to 2.1 kg mm^{-2} and the temperature range of 878 to 1026° K. Lawley *et al* [43] reported on α-Fe at 857° K. Sherby and Lytton [44] collected creep data for both α- and γ-iron, including those of Feltham for γ-iron at 1214 and 1500° K. They extrapolated these data to the transformation temperature and calculations based on their extrapolation indicate that the activation area-stress relation seems to remain unchanged through the transformation.

For Fe–3.1% Si, Barrett [45] covered a range of stress from 0.1 to 2 kg mm^{-2} at 1093 and 1298° K. He included also some earlier results of Lytton on the same material at 913° K. The results on Fe–Al alloys with Al ranging from 19.4 to 25.5% were taken from the data of Lawley *et al* [43] at 900° K. Also shown in fig. 12 are the activation areas of an austenitic Fe-based alloy at 977° K based on data reported by Garofalo *et al* [46]. The grain size in their specimens ranged from 9 to 190 μm and yet the activation area-stress relation does not seem to be affected. In 304 stainless steel, Cuddy [8] observed that secondary creep rate is uniquely related to effective stress (applied stress minus internal stress) although specimens were subjected to different thermomechanical histories leading to different internal stresses and substructures. The activation areas calculated from these data are also shown in fig. 12. It is seen that the correlation still holds after correction for the internal stress.

3.11. Bcc Metals, Fe, Ta, Nb, Mo, and W

Fig. 13 shows the activation areas for bcc metals. Data for Fe are those of Ishida *et al* [42] mentioned before. Data for W are those of Klopp *et al* [47] at 1366 and 2477° K. Carvalhinhos and Argent [48] studied Mo at 1373 to 1513° K., while Rawson and Argent [49] studied Nb at 1223 to 1273° K. Titran [50] reported on Ta-alloy (T-222) at 1366 to 1700° K and Green [51] reported on Ta at 1963 to 2923° K.

Low-temperature deformation of bcc metals was discussed by Conrad and Hayes [1] who collected all the data and calculated activation area (activation volume in their terminology) as a function of effective stress (applied stress minus internal stress). Their collection can be grouped into the region between the dotted lines in fig. 13. It is seen that such a region is clearly separated

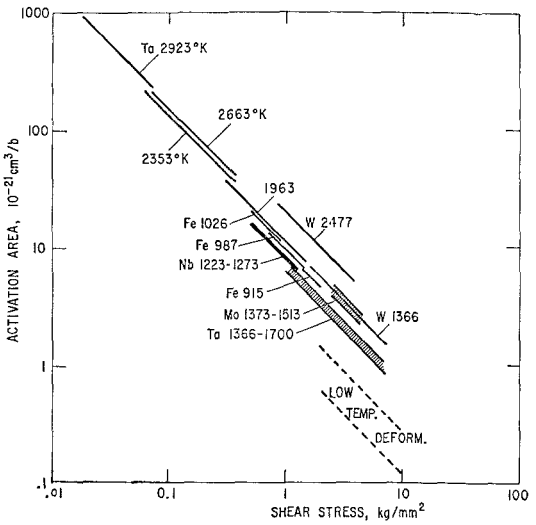

Figure 13 Activation area for the creep of body-centred-cubic metals.

from the activation areas in high temperature creep. The flow stress temperature curve also shows two separate regions. A correction for internal stress still has to be made in the case of high-temperature creep but it does not seem to affect the correlation as shown in the case of 304 stainless steel. In any case, it does not seem likely that the activation areas for low-temperature deformation and high-temperature creep would merge. Until such a merger is found the mechanism for high-temperature creep is believed to be different from that of low-temperature deformation which is widely accepted as the Peierls mechanism for bcc metals.

3.12. All Materials, a General Correlation

No attempt was made to collect all creep data in the previous plots. However, the apparent direct relation between activation area and stress and the fact that such a relation does not seem to be affected by many material variables prompted us to suggest a general correlation between activation area and stress for all materials. This is shown in fig. 14. It is seen that within a scatter of $\pm$ 0.5 the logarithms of the activation areas of all materials lie on a straight line (with a slope of about -0.9) when plotted against the logarithm of the stress*. In view of the variety of materials, compositions, grain sizes, and temperatures, such a correlation is quite remarkable. It seems to imply the existence of a single dislocation mechanism operative in all crystalline materials.

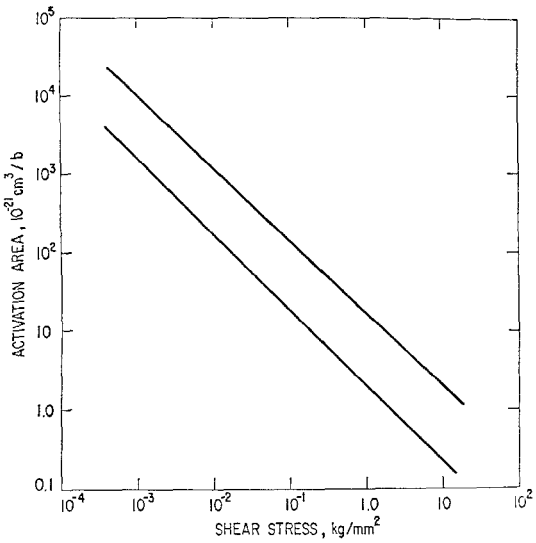

Figure 14 Activation area for the creep of all metals, alloys, semiconductors and ionic solids.

4. Discussion

Most existing theories [52-57] on the non-linear stress-dependence of steady state creep rate require variations of microstructure with stress; for example, in early theories of Weertmen [52-54] the width of pile-ups, the subgrain size, and the distance between pile-up groups are all functions of stress. Such structural variations are still required in his new theories [56] of creep. Barrett and Nix [57] suggested that the density of mobile dislocation varies with the 3rd power of stress, while Weertman and Weertman [55] preferred a 2nd power of stress. Nabarro [58] estimated that the steady state length of link in the dislocation network varies as $1/\sigma$. All these can be classified as "structure theories" of steady state creep. In this class of theories, the fundamental rate mechanism such as the climb of dislocations, or the diffusion of vacancies, is considered to be linear with stress. The non-linearity arises from the microstructural variations with stress.

These "structure theories" are supported by direct observations such as the subgrain size [56] which varies with $1/\sigma$ and the dislocation density [57] which varies with σ^3 in steady state creep. Sometimes the generality of the stress-depend-

*Calculations based on recent data [81, 82] indicate that the correlation holds good for creep of UC and ZrC also.

ence of microstructure is questioned [45]. The main difficulty with the structure theory is that the non-linear stress-dependence of creep rate is observed not only under conditions in which each specimen is crept until the steady state is reached, but also under conditions in which the stress is suddenly changed so that the microstructure is maintained essentially constant. Many examples of these "stress change" tests are available [8, 13, 59, 61]. They are ignored probably because of the difficulty in conceiving that the velocity of dislocations could have a non-linear stress-dependence.

However, non-linear stress-dependence of dislocation velocity at low temperatures is well accepted [62-65]. Application of such dependence to the stress-dependence of strain rate is also well known [66, 67]. Numerous theories [2, 36, 68] have been proposed for such non-linear behaviour. Yet very few theories [76, 69] of this nature are intended for high-temperature deformation. They could be classified as "mobility theories" for steady state creep. In view of the fact that the velocity of dislocations varies non-linearly with stress at low temperatures, it seems unnecessary to exclude this possibility for high-temperature behaviour. Some recent experiments [70, 71] on the effect of driving force on the mobility of tilt boundaries in Al seem to suggest such a possibility. The non-linear behaviour there cannot be easily attributed to structural variations. It seems more reasonable to rationalise such behaviour in terms of the mobility of dislocations.

Since the calculation of activation area involves the assumption of constant structure, the present analysis belongs to the mobility theories. However, it is not a mechanistic theory except that it requires the motion of dislocations. Such motion could be slip or climb and could involve obstacles such as impurities, fine particles, jogs, nodes, or other dislocations. The problem is to find a specific mechanism which is consistent with the activation area-stress relationship just presented.

It is not the purpose of this paper to discuss such mechanisms. However, it suffices to point out that a jog-limited motion of dislocations [72] with a distribution of jog-spacings could produce such an activation area-stress relationship. Since the diffusion of jogs is the rate-limiting step, both the activation enthalpy and the activation volume should be similar to those for self-diffusion.

Some limitations of the jog-dragging model have been discussed recently by Weertman [56, 73, 74]. Although there seems to be no serious objection to the model, some refinement could be achieved by examining the details. Firstly, Cottrell's theory [75] does not rule out the possibility that jogs of opposite signs are nearly equal in number. Jogs are produced not only by intersecting screw dislocations, but also [76, 77] by cross-slip, by cutting through a network, or by the condensation of vacancies. In all these latter cases, equal numbers of jogs of opposite signs are produced. As pointed out by Weertman, although long screw dislocations may contain a net number of jogs of one sign (this net number is small, compared to the total number of jogs on the dislocation), short segments may contain a number of either sign. In other words, jogs of opposite signs are about equal in number everywhere although there may be a net number of one sign in some regions and of the other sign in other regions. Secondly, when a dislocation contains equal numbers of jogs of opposite signs, it is not necessarily true that core diffusion takes place. It still depends on whether the time required for diffusion between jogs of opposite signs is shorter along the dislocation or through the lattice. Furthermore, unless jogs of alternate signs are arranged along the dislocation, a group of even three jogs of one sign can move only by bulk diffusion of vacancies. Thirdly, the jog-dragging model is associated with a complicated diffusion problem [57, 77-80]. However, because of the existence of jogs of both signs, the local concentration of vacancies is probably not greatly different from the equilibrium value. This is indicated in the stress-change experiments and the fact that the activation enthalpy is very close to that of self-diffusion.

5. Summary and Conclusions

(i) The activation area for creep, as for low-temperature deformation, is strongly dependent on stress and weakly dependent on temperature, composition, grain size, crystal structure and other material variables.

(ii) Within a scatter of ± 0.5 there is a correlation between the logarithm of activation area and the logarithm of shear stress for all metals, alloys, semiconductors, and ionic crystals so far examined.

(iii) A jog-limited motion of dislocations with a distribution of jog-spacings is consistent with

this correlation. Some objections to the jog mechanism are discussed.

Acknowledgement

This work was partially supported by Army Research Office, Durham, North Carolina, under contract DA-31-124-ARO (D)-382. The authors thank Professor M. Gensamer for his interest and advice.

References

1. H. CONRAD and W. HAYES, *Trans. ASM* **56** (1963) 249.
2. J. E. DORN and S. RAJNAK, *Trans TMS-AIME* **230** (1964) 1052.
3. J. E. DORN, "Creep and Recovery" (Am. Soc. Metals, Metals Park, Ohio, 1957) p. 255.
4. G. T. CHEVALIER, P. MCCORNICK, and A. L. RUOFF, *J. Appl. Phys.* **38** (1967) 3697.
5. J. C. M. LI, "Dislocation Dynamics", edited by A. R. Rosenfield *et al* (McGraw-Hill, New York, 1968) p. 87.
6. F. R. N. NABARRO, in "Strength of Solids" (The Physical Society, London, 1948) p. 75.
7. C. HERRING, *J. Appl. Phys.* **21** (1950) 437.
8. L. J. CUDDY, *Met. Trans.* **1** (1970) 395.
9. J. WEERTMAN, *ibid* **218** (1960) 207.
10. *Idem, J. Mech. Phys. Solids* **4** (1956) 230.
11. J. H. HARPER and J. E. DORN, *Acta Met.* **5** (1959) 654.
12. I. S. SERVI and N. J. GRANT, *Trans. TMS-AIME* **191** (1951) 917.
13. S. K. MITRA and D. MCLEAN, *Met. Sci. J.* **1** (1967) 192.
14. H. LAKS, C. D. WISEMAN, O. D. SHERBY, and J. E. DORN, Institute of Eng. Res., University of California, Series No. 22, Issue 37 (1954).
15. S. DUSHMAN, L. W. DUNBAR, and H. HUTHSTEINER, *J. Appl. Phys.* **15** (1944) 108.
16. J. E. DORN, NPL Conference on Creep and Fracture, (Philosophical Library, Inc., New York, 1957) p. 89.
17. C. R. BARRETT and O. D. SHERBY, *Trans. TMS-AIME* **230** (1964) 1322.
18. P. FELTHAM and J. D. MEAKIN, *Acta Met.* **7** (1959) 614.
19. R. M. BONESTEEL and O. D. SHERBY, *ibid* **14** (1966) 385.
20. P. FELTHAM and G. J. COPLEY, *Phil. Mag.* **5** (1960) 649.
21. M. HERMAN and N. BROWN, *Trans. TMS-AIME* **206** (1956) 604.
22. N. BROWN and D. R. LENTON, *Acta Met.* **17** (1969) 669.
23. O. D. SHERBY, *Trans. TMS-AIME* **212** (1958) 708.
24. D. E. MUNSON and R. A. HUGGINS, DMS Rept., No. 63-4, Stanford University (1963).
25. E. M. HOWARD, W. L. BARMORE, J. D. MOTE, and J. E. DORN, *Trans. TMS-AIME* **227** (1963) 1061.
26. J. WEERTMAN and P. SHAHNIAN, *ibid* **206** (1956) 1223.
27. J. P. DENNISON, R. J. LLEWELLYN, and B. WILSHIRE, *J. Inst. Met.* **95** (1967) 115.
28. C. M. SELLARS and A. G. QUARRELL, *ibid* **90** (1961) 329.
29. C. A. PAMPILLO and A. E. VIDOZ, *Acta Met.* **14** (1966) 313.
30. MCG. TEGART and O. D. SHERBY, *Phil. Mag.* **3** (1958) 1287.
31. MCG. TEGART, *Acta Met.* **9** (1961) 614.
32. J. E. FLINN and D. E. MUNSON, *Phil. Mag.* **10** (1964) 861.
33. J. E. FLINN and S. A. DURAN, *Trans. TMS-AIME* **236** (1966) 1056.
34. W. D. G. BENNETT and G. SUMMER, "The Metallurgy of Beryllium" (The Inst. of Metals, London, 1963) p. 177.
35. A. J. ARDELL and O. D. SHERBY, *Trans. TMS-AIME* **239** (1967) 1547.
36. A. J. ARDELL, *J. Appl. Phys.* **37** (1966) 2910.
37. J. J. GILMAN, *ibid* **36** (1965) 3195.
38. I. M. BERNSTEIN, *Trans. TMS-AIME* **239** (1967) 1518.
39. R. W. CHRISTY, *Acta Met.* **2** (1954) 284.
40. P. HAASEN, *Trans. Faraday Soc.* **38** (1964) 191.
41. E. PEISSKER, P. HAASEN, and H. ALEXANDER, *Phil. Mag.* 7 (1962) 1279.
42. Y. ISHIDA, C. Y. CHENG, and J. E. DORN, *Trans. TMS-AIME* **236** (1966) 964.
43. A. LAWLEY, J. A. COLL, and R. W. CAHN, *ibid* **218** (1960) 166.
44. O. D. SHERBY and J. L. LYTTON, *ibid* **206** (1956) 928.
45. C. R. BARRETT, *ibid* **239** (1967) 1726.
46. F. GAROFALO, W. D. DOMIS, and F. VON GEMMINGEN, *ibid* **230** (1964) 1460.
47. W. D. KLOPP, W. R. WITZKE, and P. O. RAFFO, *ibid* **233** (1965) 1560.
48. H. CARVALHINHOS and B. B. ARGENT, *J. Inst. Met.* **95** (1967) 364.
49. J. D. W. RAWSON and B. B. ARGENT, *J. Inst. Met.* **95** (1967) 212.
50. R. H. TITRAN, *AIME, Abs. Bulletin* **2** (1967) No. 2, 91.
51. W. V. GREEN, *Trans. TMS-AIME* **223** (1965) 1818.
52. J. WEERTMAN, *J. Appl. Phys.* **26** (1955) 1213.
53. *Idem, ibid* **28** (1957) 362.
54. *Idem, ibid* **28** (1957) 1185.
55. J. WEERTMAN and J. R. WEERTMAN in "Physical Metallurgy", edited by R. W. Cahn (North-Holland Publishing Co., Amsterdam, 1965) p. 793.
56. J. WEERTMAN, *Trans. ASM* **61** (1968) 681.
57. C. R. BARRETT and W. D. NIX, *Acta Met.* **13** (1965) 1247.
58. F. R. N. NABARRO, *Phil. Mag.* **16** (1967) 231.
59. O. D. SHERBY, T. A. TROZERO, and J. E. DORN, *Proc. ASTM* **56** (1956) 789.

60. B. Y. CHIROUZE, D. M. SCHWARTZ, and J. E. DORN, *Trans. ASM* **60** (1967) 51.
61. D. R. CROPPER and T. G. LANGDON, *Phil. Mag.* **18** (1968) 1181.
62. W. G. JOHNSTON and J. J. GILMAN, *J. Appl. Phys.* **30** (1959) 129.
63. D. F. STEIN and J. R. LOW JR., *ibid* **31** (1960) 362.
64. H. W. SCHADLER, *Acta Met.* **12** (1964) 861.
65. H. D. GUBERMAN, *ibid* **16** (1968) 713.
66. W. G. JOHNSTON and D. F. STEIN, *ibid* **11** (1963) 317.
67. J. C. M. LI, *Can. J. Phys.* **45** (1967) 493.
68. R. L. FLEISCHER, *J. Appl. Phys.* **33** (1962) 3504.
69. J. C. M. LI, *Trans. TMS-AIME* **227** (1963) 1474.
70. B. B. RATH and H. HU, *ibid* **245** (1969) 1577.
71. J. C. M. LI, *ibid* **245** (1969) 1591.
72. *Idem, Trans. ASM* **61** (1968) 699.
73. J. WEERTMAN, *Trans. TMS-AIME* **233** (1965) 2069.
74. *Idem, Acta Met.* **15** (1967) 1081.
75. A. H. COTTRELL, "Dislocations and Mechanicai Properties of Crystals", edited by J. C. Fisher *et al* (Wiley, New York, 1957) p. 509.
76. G. B. GIBBS, *Scripta Met.* **1** (1967) 135.
77. W. D. NIX, *Acta Met.* **15** (1967) 1079.
78. J. J. HOLMES, *ibid* **15** (1967) 570.
79. P. CHAUDHARI, *Scripta Met.* **1** (1967) 145.
80. W. D. NIX, *ibid* **1** (1967) 171.
81. R. CHANG, *J. Appl. Phys.* **33** (1962) 858.
82. D. W. LEE and J. S. HAGGERTY, *J. Amer. Cer. Soc.* **52** (1969) 641.

Received 15 December 1969 and accepted 18 February 1970.